

Magnetic field distributions around superconducting strips on ferromagnetic substrates

Yasunori Mawatari

National Institute of Advanced Industrial Science and Technology (AIST), Tsukuba, Ibaraki 305-8568, Japan

(Received 10 October 2007; published 4 March 2008)

The complex-field approach is developed to derive analytical expressions of the magnetic field distributions around superconducting strips on ferromagnetic substrates (SC/FM strips). We consider the ferromagnetic substrates as ideal soft magnets with an infinite magnetic permeability, neglecting the ferromagnetic hysteresis. On the basis of the critical state model for a superconducting strip, the ac susceptibility $\chi'_1 + i\chi''_1$ of a SC/FM strip exposed to a perpendicular ac magnetic field is theoretically investigated, and the results are compared with those for superconducting strips on nonmagnetic substrates (SC/NM strips). The real part χ'_1 for $H_0/j_c d_s \rightarrow 0$ (where H_0 is the amplitude of the ac magnetic field, j_c is the critical current density, and d_s is the thickness of the superconducting strip) of a SC/FM strip is 3/4 of that of a SC/NM strip. The imaginary part χ''_1 (or ac loss Q) for $H_0/j_c d_s < 0.14$ of a SC/FM strip is larger than that of a SC/NM strip, even when the ferromagnetic hysteresis is neglected, and this enhancement of χ''_1 (or Q) is due to the edge effect of the ferromagnetic substrate.

DOI: 10.1103/PhysRevB.77.104505

PACS number(s): 74.25.Nf, 74.25.Ha, 74.25.Sv, 74.78.-w

I. INTRODUCTION

High-temperature superconducting coated conductors have been developed for applications in electric power devices (e.g., power cable, transformer, motor, fault current limiter, cryocooler, and so on), and remarkable progress toward high-current and long-length conductors has recently been reported.¹ In superconducting coated conductors, the superconducting layers are generally fabricated on metallic substrates with oxide buffer layers, and ferromagnetic materials (e.g., Ni alloys) are promising candidates for the metallic substrates.^{2,3} The magnetic behavior of ferromagnetic substrates can strongly affect the electromagnetic response of superconducting coated conductors. Although the effects of ferromagnetic substrates on ac losses of superconducting coated conductors have been extensively investigated experimentally and numerically,⁴⁻¹³ ac losses in superconducting strips on ferromagnetic substrates have not been investigated analytically. Genenko *et al.*¹⁴ analytically investigated the magnetic field and current distributions in superconducting strips surrounded by soft magnets, but they did not consider realistic geometries similar to those of coated conductors.

In the present paper, we develop a theoretical framework to investigate electromagnetic response of superconducting strips on ferromagnetic substrates (SC/FM strips), and we compare the results with those for superconducting strips on nonmagnetic substrates (SC/NM strips).¹⁵⁻¹⁷ Section II introduces the theoretical models and methods that we used to investigate the magnetic field around SC/FM strips. Section III gives the theoretical results for the magnetic field distribution around a SC/FM strip in which the superconducting strip is in the ideal Meissner state and exposed either to a perpendicular magnetic field, a parallel magnetic field, or a transport current. Section IV gives the theoretical results for dc and ac responses of a SC/FM strip in which the superconducting strip is in the critical state and the SC/FM strip is exposed to a perpendicular magnetic field. Section V describes the comparison of our theoretical results with experimental data by Suenaga *et al.*¹³ and summarizes our results.

II. MODEL

In this section, the configuration of a SC/FM strip is defined, and the basic theoretical models used to investigate the electromagnetic response of a SC/FM strip are introduced.

Consider a SC/FM strip of width $2a$, total thickness $d_s + d_m$, and infinite length along the z axis, as shown in Fig. 1. This strip consists of a superconducting strip whose thickness is d_s , and a ferromagnetic substrate whose thickness is d_m , where $d_s + d_m \ll 2a$. Let $\epsilon \equiv \max(d_s, d_m)$ be a positive infinitesimal, and the thin strip limit of $\epsilon \rightarrow +0$ enables analytical expressions of the magnetic field distribution around a SC/FM strip to be derived as follows.

A. Complex field

To analyze a two-dimensional magnetic field, $\mathbf{H} = H_x(x, y)\hat{x} + H_y(x, y)\hat{y}$, we consider the complex field¹⁸⁻²⁷

$$\mathcal{H}(\zeta) = H_y(x, y) + iH_x(x, y), \quad (1)$$

which is the analytical function of the complex variable $\zeta = x + iy$ outside of a SC/FM strip. Applying Cauchy's integral formula²⁸ to $\mathcal{H}(\zeta)$ yields the following:

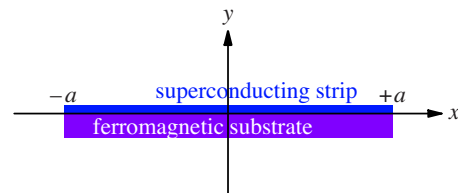


FIG. 1. (Color online) Cross section of a SC/FM strip in the xy plane. Superconducting strip is situated at $|x| < a$ and $0 < y < d_s$, and ferromagnetic substrate at $|x| < a$ and $-d_m < y < 0$, where $d_s + d_m \ll 2a$.

$$\begin{aligned}
\mathcal{H}(\zeta) &= \frac{1}{2\pi i} \oint_C d\zeta' \frac{\mathcal{H}(\zeta')}{\zeta' - \zeta} \\
&= \lim_{R \rightarrow \infty} \frac{1}{2\pi} \int_0^{2\pi} d\theta \frac{Re^{i\theta} \mathcal{H}(Re^{i\theta})}{Re^{i\theta} - \zeta} \\
&\quad + \frac{1}{2\pi i} \int_{-\infty}^{+\infty} dx' \frac{\mathcal{H}(x' + i\epsilon) - \mathcal{H}(x' - i\epsilon)}{x' - \zeta}, \quad (2)
\end{aligned}$$

where the closed contour C has three components: a line just above the real axis (i.e., $\zeta' = x' + i\epsilon$ from $x' = -\infty$ to $x' = +\infty$), an infinite circle (i.e., $\zeta' = Re^{i\theta}$ from $\theta = 0$ to $\theta = 2\pi$ with $R \rightarrow \infty$), and a line just below the real axis (i.e., $\zeta' = x' - i\epsilon$ from $x' = +\infty$ to $x' = -\infty$), see Fig. 7 in Ref. 26. Substitution of $\mathcal{H}(\zeta) \rightarrow H_{ay} + iH_{ax}$ for $|\zeta| \rightarrow \infty$ and $\mathcal{H}(x' + i\epsilon) = \mathcal{H}(x' - i\epsilon)$ for $|x'| > a$ into Eq. (2) leads to the generalized Biot-Savart law for a SC/FM strip:

$$\mathcal{H}(\zeta) = (H_{ay} + iH_{ax}) + \frac{1}{2\pi} \int_{-a}^{+a} dx' \frac{K_z(x') + i\sigma_m(x')}{\zeta - x'}, \quad (3)$$

where $\mathbf{H}_a = H_{ax}\hat{x} + H_{ay}\hat{y}$ is a uniform applied magnetic field, $K_z(x)$ is the sheet current in a superconducting strip, and $\sigma_m(x)$ is the effective sheet magnetic charge²⁹ in a ferromagnetic substrate. The $K_z(x)$ and $\sigma_m(x)$ are defined by

$$K_z(x) = H_x(x, -\epsilon) - H_x(x, +\epsilon), \quad (4)$$

$$\sigma_m(x) = H_y(x, +\epsilon) - H_y(x, -\epsilon), \quad (5)$$

respectively. The net magnetic charge is zero; that is, $\int_{-a}^{+a} \sigma_m(x) dx = 0$.

The multipole expansion of Eq. (3) for $|\zeta|/a \rightarrow \infty$ is given by²⁵

$$\mathcal{H}(\zeta) \rightarrow (H_{ay} + iH_{ax}) + \frac{I_z}{2\pi\zeta} + \frac{-m_y + im_x}{2\pi\zeta^2} + \dots, \quad (6)$$

where $I_z = \int_{-a}^{+a} K_z(x) dx$ is the transport current flowing in a superconducting strip. The $\mathbf{m} = m_x\hat{x} + m_y\hat{y}$ is the magnetic moment per unit length of a SC/FM strip:

$$m_y = - \int_{-a}^{+a} dx x K_z(x) = \int_{-a}^{+a} dx x [H_x(x, +\epsilon) - H_x(x, -\epsilon)], \quad (7)$$

$$m_x = \int_{-a}^{+a} dx x \sigma_m(x) = \int_{-a}^{+a} dx x [H_y(x, +\epsilon) - H_y(x, -\epsilon)]. \quad (8)$$

The m_y is induced by $K_z(x)$ in a superconducting strip, whereas m_x is induced by $\sigma_m(x)$ in a ferromagnetic substrate.

The complex potential defined by

$$\mathcal{G}(\zeta) = \int \mathcal{H}(\zeta) d\zeta \quad (9)$$

is convenient for visualizing the magnetic field lines around a SC/FM strip, because the contour lines of the real part of Eq. (9), $\text{Re } \mathcal{G}(\zeta)$, correspond to the magnetic field lines.^{26,27}

The variable transformation (i.e., the conformal mapping) defined by

$$\eta = i\sqrt{\zeta^2 - a^2}, \quad \zeta = -i\sqrt{\eta^2 - a^2} \quad (10)$$

is useful for analyzing $\mathcal{H}(\zeta)$ for a SC/FM strip.

B. Ferromagnetic substrate

The ferromagnetic materials (e.g., Ni-W alloys) used as metal substrates for coated conductors are classified as soft magnets.^{3,7} For simplicity, in the present paper, we consider the ferromagnetic substrates as *ideal soft magnets*, in which the relationship between the magnetic induction \mathbf{B} and the magnetic field \mathbf{H} is given by¹⁴ $\mathbf{B} = \mu_m \mathbf{H}$, where μ_m is much larger than the magnetic permeability of the vacuum μ_0 (i.e., $\mu_m/\mu_0 \gg 1$). Also, in the ideal soft magnet model, we neglect the ferromagnetic hysteresis and assume that the saturation field H_s is much larger than $|\mathbf{H}|$.

In the infinite-permeability limit ($\mu_m/\mu_0 \rightarrow \infty$), the $\mathbf{H} = \mathbf{B}/\mu_0$ outside of the ideal soft magnet has only a perpendicular component at the surface.²⁹ Therefore, the boundary condition at the surface of a ferromagnetic substrate (i.e., at $y = -\epsilon$) is given by

$$H_x(x, -\epsilon) = \text{Im } \mathcal{H}(x - i\epsilon) = 0 \quad \text{for } |x| < a. \quad (11)$$

The magnetic field distribution for a large but finite permeability ($\mu_m/\mu_0 \gg 1$) is not significantly different from that for an infinite permeability ($\mu_m/\mu_0 \rightarrow \infty$).¹⁴ The simple boundary condition of Eq. (11) thus enables analytical expressions of $\mathcal{H}(\zeta)$ to be derived.

C. Superconducting strip

The ideal Meissner state model (Sec. III) and the critical state model (Sec. IV) are adopted to investigate the electromagnetic response of a superconducting strip in a SC/FM strip.

In Sec. III, the ideal case is considered, namely, when a superconducting strip is in the ideal Meissner state. In this state, the magnetic flux does not penetrate a superconducting strip, and consequently, the perpendicular component of the magnetic field vanishes, that is, $H_y(x, +\epsilon) = 0$.

In Sec. IV, a more realistic case is considered, and thus we used the critical state model with constant critical current density j_c , as in the Bean model.³⁰ Similar to earlier calculations,¹⁵⁻¹⁷ the effects of the lower critical field H_{c1} are neglected (i.e., $H_{c1} \ll |\mathbf{H}|$), and thus the $\mathbf{B} - \mathbf{H}$ relationship is simply given by $\mathbf{B} = \mu_0 \mathbf{H}$. In the critical state model, the magnetic flux penetrates and K_z reaches its critical value $j_c d_s$ near the edges of the superconducting strip. The $|K_z(x)| = j_c d_s$ holds in the flux-filled region [where $H_y(x, +\epsilon) \neq 0$] near the edges in a superconducting strip, whereas the flux-free region [where $H_y(x, +\epsilon) = 0$] exists near the center of a superconducting strip.

III. IDEAL MEISSNER STATE

In this section, we consider the complex field $\mathcal{H}(\zeta)$ for a SC/FM strip in which the superconducting strip is in the

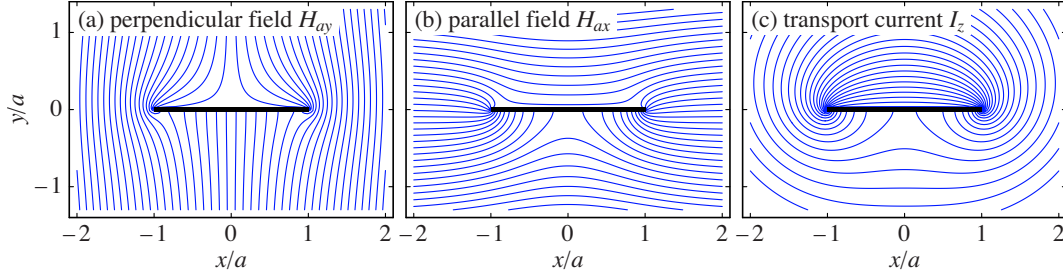


FIG. 2. (Color online) Magnetic field lines [i.e., contour lines of $\text{Re } \mathcal{G}(\zeta)$] around a SC/FM strip in which the superconducting strip is in the ideal Meissner state: (a) in a perpendicular magnetic field H_{ay} , (b) in a parallel magnetic field H_{ax} , and (c) with a transport current I_z . Thick horizontal bar at $-1 < x/a < 1$ and $y=0$ denotes the SC/FM strip.

ideal Meissner state. In the ideal Meissner state, the magnetic field component perpendicular to the surface of the superconducting strip at $y=+\epsilon$ is zero:

$$H_y(x, +\epsilon) = \text{Re } \mathcal{H}(x + i\epsilon) = 0 \quad \text{for } |x| < a. \quad (12)$$

In addition to the boundary conditions given by Eqs. (11) and (12), further conditions depending on H_{ax} , H_{ay} , and I_z are needed to determine $\mathcal{H}(\zeta)$, as shown in the following subsections. The derivation of $\mathcal{H}(\zeta)$ is shown in Appendix A, and the details of the square root functions are shown in Appendix B.

A. Response to a perpendicular magnetic field

Here, the $\mathcal{H}(\zeta)$ for a SC/FM strip is presented for the case when a SC/FM strip is exposed to a perpendicular magnetic field $\mathbf{H}_a = H_{ay}\hat{y}$; that is, when $H_{ay} \neq 0$ and $H_{ax} = I_z = 0$.

The corresponding complex field for $H_{ax} = I_z = 0$, which satisfies the conditions given in Eqs. (11) and (12), is expressed as

$$\mathcal{H}(\zeta) = H_{ay} \left(1 - \frac{a}{2\eta} \right) \sqrt{\frac{\eta+a}{\eta}}, \quad (13)$$

where $\eta = \eta(\zeta)$ is a function of ζ given by Eq. (10). Equation (13) is expanded for $|\zeta| \sim |\eta| \rightarrow \infty$ as

$$\mathcal{H}(\zeta) \rightarrow H_{ay} \left(1 + \frac{3a^2}{8\zeta^2} + \dots \right). \quad (14)$$

Comparison of Eqs. (6) and (14) yields the magnetic moment per unit length,

$$m_y = \chi_{0y} H_{ay}, \quad (15)$$

where χ_{0y} is the magnetic susceptibility given by

$$\chi_{0y} = -(3\pi/4)a^2. \quad (16)$$

Here, we defined χ_{0y} as the ratio of m_y in units of (A m) to H_{ay} in units of (A/m), such that χ_{0y} is in units of (m^2). Equation (16) corresponds to 3/4 of the magnetic susceptibility of a SC/NM strip in the ideal Meissner state,¹⁶ $\chi_{0y} = -\pi a^2$.

The complex potential calculated by substituting Eq. (13) into Eq. (9) is given by

$$\mathcal{G}(\zeta) = -iH_{ay} \sqrt{\eta(\eta+a)}. \quad (17)$$

Figure 2(a) shows the magnetic field lines calculated from

$\text{Re } \mathcal{G}(\zeta)$ with Eqs. (10) and (17). At the surface of the ferromagnetic substrate at $y=-\epsilon$, the \mathbf{H} near the edges is *downward* [i.e., $H_y(x, -\epsilon) < 0$ when $H_{ay} > 0$] for $x_p < |x| < a$, whereas \mathbf{H} is mostly *upward* [i.e., $H_y(x, -\epsilon) > 0$ when $H_{ay} > 0$] for $|x| < x_p$, where $x_p/a = \sqrt{3}/2 = 0.866$. Such pronounced behavior in \mathbf{H} due to a ferromagnetic substrate results in the concentration of the magnetic field near the edges of the SC/FM strip.

B. Response to a parallel magnetic field

Here, the $\mathcal{H}(\zeta)$ for a SC/FM strip is presented for the case when a SC/FM strip is exposed to a parallel magnetic field $\mathbf{H}_a = H_{ax}\hat{x}$; that is, when $H_{ax} \neq 0$ and $H_{ay} = I_z = 0$.

The corresponding complex field for $H_{ay} = I_z = 0$, which satisfies the conditions given in Eqs. (11) and (12), is expressed as

$$\mathcal{H}(\zeta) = iH_{ax} \left(1 + \frac{a}{2\eta} \right) \sqrt{\frac{\eta-a}{\eta}}, \quad (18)$$

where η is a function of ζ by Eq. (10). Equation (18) is expanded for $|\zeta| \sim |\eta| \rightarrow \infty$ as

$$\mathcal{H}(\zeta) \rightarrow iH_{ax} \left(1 + \frac{3a^2}{8\zeta^2} + \dots \right). \quad (19)$$

Comparison of Eqs. (6) and (19) yields the magnetic moment per unit length,

$$m_x = \chi_{0x} H_{ax}, \quad (20)$$

where χ_{0x} is the magnetic susceptibility given by

$$\chi_{0x} = +(3\pi/4)a^2. \quad (21)$$

Equation (21) corresponds to 3/4 of the magnetic susceptibility of a ferromagnetic strip without a superconducting strip, $\chi_{0x} = +\pi a^2$.

The complex potential calculated by substituting Eq. (18) into Eq. (9) is given by

$$\mathcal{G}(\zeta) = H_{ax} \sqrt{\eta(\eta+a)}. \quad (22)$$

Figure 2(b) shows the magnetic field lines calculated from Eqs. (10) and (22). At the surface of the superconducting strip at $y=+\epsilon$, the \mathbf{H} near the edges is *leftward* [i.e., $H_x(x, +\epsilon) < 0$ when $H_{ax} > 0$] for $x_p < |x| < a$, whereas \mathbf{H} is mostly

rightward [i.e., $H_x(x, +\epsilon) > 0$ when $H_{ax} > 0$] for $|x| < x_p$, where $x_p/a = \sqrt{3}/2 = 0.866$.

C. Response to a transport current

Here, the $\mathcal{H}(\zeta)$ for a SC/FM strip is presented for the case when a superconducting strip in a SC/FM strip carries a transport current I_z ; that is, when $I_z \neq 0$ and $H_{ax} = H_{ay} = 0$.

The corresponding complex field for $H_{ax} = H_{ay} = 0$, which satisfies the boundary conditions given in Eqs. (11) and (12), is expressed as

$$\mathcal{H}(\zeta) = i \frac{I_z}{2\pi\eta} \frac{1}{\eta} \sqrt{\frac{\eta - a}{\eta}}, \quad (23)$$

where η is a function of ζ by Eq. (10). Equation (23) is expanded for $|\zeta| \sim |\eta| \rightarrow \infty$ as

$$\mathcal{H}(\zeta) \rightarrow \frac{I_z}{2\pi} \left(\frac{1}{\zeta} + \frac{ia}{2\zeta^2} + \dots \right). \quad (24)$$

Comparison of Eqs. (6) and (24) reveals that, despite $H_{ax} = 0$, the magnetic moment per unit length,

$$m_x = aI_z/2, \quad (25)$$

is induced from I_z .

The complex potential calculated by substituting Eq. (23) into Eq. (9) is given by

$$\mathcal{G}(\zeta) = (I_z/\pi) \operatorname{arcsinh}(\sqrt{\eta/a}). \quad (26)$$

Figure 2(c) shows the magnetic field lines calculated from Eqs. (10) and (26).

IV. CRITICAL STATE

In this section, we consider $\mathcal{H}(\zeta)$ for a SC/FM strip in which the superconducting strip is in the critical state. A SC/FM strip is exposed to a perpendicular magnetic field $\mathbf{H}_a = H_{ay} \hat{\mathbf{y}}$ and carries no net transport current (i.e., $H_{ax} = I_z = 0$), where H_{ay} is either dc or ac magnetic field.

A. Response to a dc magnetic field

Here, we consider the case when a SC/FM strip is exposed to a dc magnetic field $H_{ay} = H_0$, which is fixed after monotonically increased from $H_{ay} = 0$.

The magnetic flux penetrates the superconducting strip near the edges, and the sheet current density $K_x(x) = -H_x(x, +\epsilon)$ [from Eqs. (4) and (11)] reaches its critical value,

$$H_x(x, +\epsilon) = \operatorname{Im} \mathcal{H}(x + i\epsilon) = -\operatorname{sgn}(x)j_c d_s \quad \text{for } b_0 < |x| < a. \quad (27)$$

In contrast, the magnetic flux does not penetrate the inner region,

$$H_y(x, +\epsilon) = \operatorname{Re} \mathcal{H}(x + i\epsilon) = 0 \quad \text{for } |x| < b_0, \quad (28)$$

where b_0 is the parameter for the flux front. At the surface of the ferromagnetic substrate, the parallel component of the magnetic field is zero, as required by the boundary condition

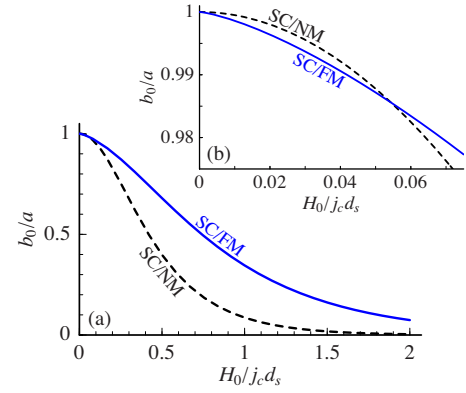


FIG. 3. (Color online) Parameter for the flux front b_0 (in units of a) as a function of an applied magnetic field H_0 (in units of $j_c d_s$) (a) for $0 < H_0/j_c d_s < 2$ and (b) for $0 < H_0/j_c d_s < 0.075$. Solid lines represent b_0 vs H_0 for a SC/FM strip obtained from Eqs. (30) and (32), and dashed lines represent b_0 vs H_0 for a SC/NM strip (Refs. 15–17).

in Eq. (11). The corresponding complex field that satisfies the conditions given in Eqs. (11), (27), and (28) is expressed by

$$\frac{\mathcal{H}(\zeta)}{2j_c d_s/\pi} = \operatorname{arctanh} \left[\sqrt{\frac{\beta_0(\eta+a)}{a(\eta+\beta_0)}} \right] - \frac{\sqrt{a\beta_0(\eta+a)(\eta+\beta_0)}}{(a+\beta_0)\eta}, \quad (29)$$

where η is given by Eq. (10), and β_0 is given by

$$\beta_0 = \sqrt{a^2 - b_0^2}. \quad (30)$$

Equation (29) is expanded for $|\zeta| \sim |\eta| \rightarrow \infty$ as

$$\frac{\mathcal{H}(\zeta)}{2j_c d_s/\pi} \rightarrow \operatorname{arctanh} \left(\sqrt{\frac{\beta_0}{a}} \right) - \frac{\sqrt{a\beta_0}}{a+\beta_0} + \frac{(a\beta_0)^{3/2}}{2(a+\beta_0)\zeta^2} + \dots \quad (31)$$

Comparison of Eqs. (6) and (31) yields the following relationship between H_0 and β_0 :

$$\frac{H_0}{2j_c d_s/\pi} = \operatorname{arctanh} \left(\sqrt{\frac{\beta_0}{a}} \right) - \frac{\sqrt{a\beta_0}}{a+\beta_0}. \quad (32)$$

The parameter for the flux front b_0 is obtained as a function of the applied magnetic field H_0 by eliminating β_0 from Eqs. (30) and (32). The resulting b_0 vs H_0 for a SC/FM strip is shown as the solid lines in Fig. 3, and $b_0 = a/\cosh(\pi H_0/j_c d_s)$ for a SC/NM strip^{15–17} is shown as the dashed lines. When $H_0/j_c d_s > 0.054$, the magnetic-flux penetration into a SC/FM strip is *slower* than that into a SC/NM strip (i.e., b_0 for a SC/FM strip is larger than b_0 for a SC/NM strip), as seen in Fig. 3(a), whereas when $H_0/j_c d_s < 0.054$, the penetration is *faster* into a SC/FM strip, as seen in Fig. 3(b).

The solid lines in Fig. 4 show the calculated distributions of $H_y(x, +\epsilon)$ and $K_z(x)$ for a SC/FM strip, and the dashed lines show H_y and K_z for a SC/NM strip.^{15–17} The $|H_y|$ and $|K_z|$ of a SC/FM strip are *smaller* than those of a SC/NM strip in the inner region ($|x|/a \lesssim 0.6$), whereas $|H_y|$ of a

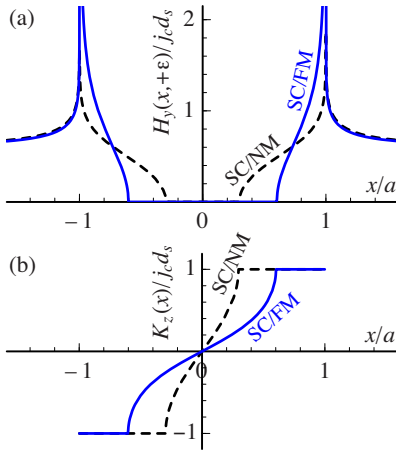


FIG. 4. (Color online) Distributions of (a) perpendicular magnetic field $H_y(x, +\epsilon)$ (in units of $j_c d_s$) and (b) sheet current $K_z(x)$ (in units of $j_c d_s$) as a function of x (in units of a) for $H_0/j_c d_s = 0.6$. Solid lines show $H_y = \text{Re} \mathcal{H}(x+i\epsilon)$ and $K_z = \text{Im}[\mathcal{H}(x-i\epsilon) - \mathcal{H}(x+i\epsilon)]$ calculated from Eq. (29) for a SC/FM strip ($b_0/a = 0.602$), and dashed lines show H_y and K_z for a SC/NM strip (Refs. 15–17) ($b_0/a = 0.297$).

SC/FM strip is *larger* in the outer region ($0.7 \lesssim |x|/a < 1$). The stronger magnetic field near the edges of a SC/FM strip is due to the edge effect of the ferromagnetic substrate, and is responsible for the faster magnetic-flux penetration (i.e., smaller b_0) into a SC/FM strip in the weak magnetic field regime ($H_0/j_c d_s < 0.054$), as shown in Fig. 3(b).

From Eqs. (6) and (31), the magnetic moment per unit length is given by $m_y = m_0(H_0)$, where

$$m_0 = -2j_c d_s \frac{(a\beta_0)^{3/2}}{a + \beta_0}. \quad (33)$$

The m_0 is obtained as a function of H_0 by eliminating β_0 in Eqs. (32) and (33) and the differential susceptibility is expressed as

$$\frac{\partial m_0}{\partial H_0} = \frac{\partial m_0 / \partial \beta_0}{\partial H_0 / \partial \beta_0} = -\frac{\pi}{4}(3a + \beta_0)(a - \beta_0). \quad (34)$$

For a weak magnetic field of $H_0 \ll j_c d_s$ (i.e., $\beta_0 \ll a$), Eq. (34) is reduced to $\partial m_0 / \partial H_0 \approx -(3\pi/4)a^2$, which corresponds to Eq. (16).

B. Response to an ac magnetic field

Here, we consider the case when a SC/FM strip is exposed to an ac magnetic field $H_{ay} = H_0 \cos \omega t$.

The magnetic moment per unit length $m_y(t)$ for an ac magnetic field is expressed as^{15,31,32}

$$m_y(t) = +m_0(H_0) - 2m_0[H_0(1 - \cos \omega t)/2], \quad (35)$$

for $0 < \omega t < \pi$, and

$$m_y(t) = -m_0(H_0) + 2m_0[H_0(1 + \cos \omega t)/2] \quad (36)$$

for $\pi < \omega t < 2\pi$, where $m_0(H_0)$ is given by Eqs. (32) and (33) by eliminating β_0 . The $m_y(t)$ can be expressed as the Fourier series:

$$\begin{aligned} m_y(t) &= H_0 \sum_{n=1}^{\infty} (\chi'_n \cos n\omega t + \chi''_n \sin n\omega t) \\ &= H_0 \sum_{n=1}^{\infty} \text{Re}[(\chi'_n + i\chi''_n)e^{-in\omega t}], \end{aligned} \quad (37)$$

where the ac susceptibility $\chi'_n + i\chi''_n$ is calculated as³³

$$\chi'_n + i\chi''_n = \frac{1}{\pi H_0} \int_0^{2\pi} d(\omega t) m_y(t) e^{in\omega t}. \quad (38)$$

Substitution of Eqs. (35) and (36) into Eq. (38) yields $\chi''_n = \chi''_n = 0$ for even n . The ac susceptibility for odd n is given by

$$\begin{aligned} \chi'_n + i\chi''_n &= \frac{2}{\pi H_0} \int_0^{\pi} d\theta e^{in\theta} [m_0(H_0) - 2m_0(H_0(1 - \cos \theta)/2)] \\ &= \frac{4}{in\pi H_0} \int_0^{H_0} dh \exp\left[in \arccos\left(1 - \frac{2h}{H_0}\right)\right] \frac{\partial m_0(h)}{\partial h}. \end{aligned} \quad (39)$$

When $H_0 \rightarrow 0$, all components of the ac susceptibility vanish except for $\chi'_1 = (\partial m_0 / \partial H_0)_{H_0 \rightarrow 0}$. The ac loss of a SC/FM strip per unit length, Q , in an ac magnetic field is proportional to χ''_1 as³³

$$Q(H_0) = \pi \mu_0 H_0^2 \chi''_1(H_0). \quad (40)$$

Figure 5 shows the real part χ'_1 and imaginary part χ''_1 of the ac susceptibility for the fundamental frequency ($n=1$) as a function of H_0 , calculated by substituting Eqs. (32) and (33) into Eq. (39). Except when the magnetic field is strong ($H_0/j_c d_s \gg 1$), the ac susceptibility of a SC/FM strip (solid lines) is significantly different from that of a SC/NM strip (dashed lines). When $H_0/j_c d_s \lesssim 1$, the real part $-\chi'_1$ of a SC/FM strip is smaller than that of a SC/NM strip, and when $H_0/j_c d_s \ll 1$, we have $\chi'_1 / \pi a^2 = -3/4$, which corresponds to Eq. (16).

As shown in Fig. 5(b), χ''_1 of a SC/FM strip (solid line) is smaller than that of a SC/NM strip (dashed line) when $H_0/j_c d_s > 0.14$, whereas χ''_1 of a SC/FM strip is larger when $H_0/j_c d_s < 0.14$. Note that the enhancement of χ''_1 for $H_0/j_c d_s < 0.14$ is not due to the ferromagnetic hysteresis in the substrate, because we assume a linear $\mathbf{B}-\mathbf{H}$ relationship in the ferromagnetic substrate, as described in Sec. II B. When $H_0/j_c d_s \lesssim 1$, the edges of SC/FM strips play crucial roles in χ''_1 . In addition to the χ''_1 of a SC/FM strip with $a_m = a_s$ (as shown in Fig. 1), Fig. 5(b) shows χ''_1 of a SC/FM strip with $a_m > a_s$ (Fig. 6), where $2a_s$ is the width of the superconducting strip and $2a_m$ is the width of the ferromagnetic substrate (see Appendix C.) Even when the ferromagnetic substrate is only 1% wider than the superconducting strip (i.e., $a_m/a_s = 1.01$), χ''_1 is strongly affected when $H_0/j_c d_s \lesssim 0.1$. For any $H_0/j_c d_s$, χ''_1 of a SC/FM strip with $a_m/a_s = 1.1$ is smaller than that of a SC/NM strip. The dependence of χ''_1 on a_m/a_s clearly confirms that the enhancement of χ''_1 of a SC/FM strip with $a_m/a_s = 1$ for $H_0/j_c d_s < 0.14$ is due to the edge effect of a ferromagnetic substrate.

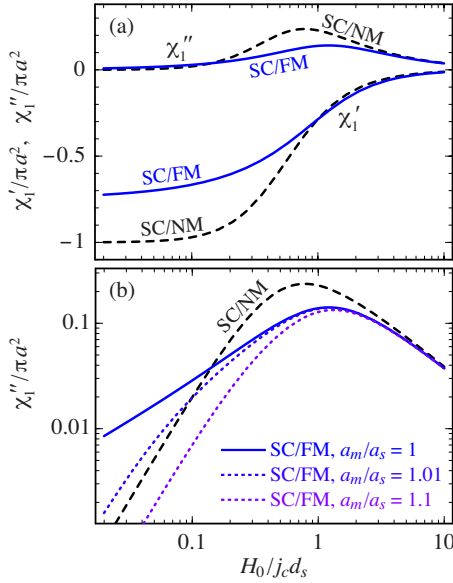


FIG. 5. (Color online) ac susceptibility $\chi'_1 + i\chi''_1$ (in units of πa^2) for the fundamental frequency ($n=1$) as a function of the amplitude of an applied ac magnetic field, H_0 , (in units of $j_c d_s$) for a SC/FM strip (solid lines) and for a SC/NM strip (dashed lines). (a) Semilog plot of the real part χ'_1 (lower lines) and imaginary part χ''_1 (upper lines) vs H_0 . (b) Log-log plot of the imaginary part χ''_1 vs H_0 for a SC/FM strip with $a_m/a_s=1$ (solid line) and for SC/FM strips with $a_m/a_s=1.01$ and 1.1 (dotted lines), where $2a_s$ is the width of the superconducting strip and $2a_m$ is the width of the ferromagnetic substrate.

V. DISCUSSION AND SUMMARY

The three key theoretical predictions presented in Sec. IV for the real part χ'_1 and imaginary part χ''_1 of the ac susceptibility, and the ac loss Q ($\propto H_0^2 \chi''_1$) of a SC/FM strip exposed to an ac perpendicular magnetic field $H_{ay} = H_0 \cos \omega t$ are as follows.

(i) The χ'_1 in the weak magnetic field limit (i.e., $\partial m_0 / \partial H_0$ for $H_0 \ll j_c d_s$) of a SC/FM strip is given by $-(3\pi/4)a^2$, which corresponds to $3/4$ of that of a SC/NM strip.

(ii) The χ'_1 of a SC/FM strip is larger (smaller) than that of a SC/NM strip in the weak (strong) field regime of $H_0/j_c d_s < 0.14$ ($H_0/j_c d_s > 0.14$), as evidenced in Fig. 5(b) by the intersection between the line for χ'_1 vs H_0 of a SC/FM strip and that of a SC/NM strip at $H_0/j_c d_s \approx 0.14$, where the inter-

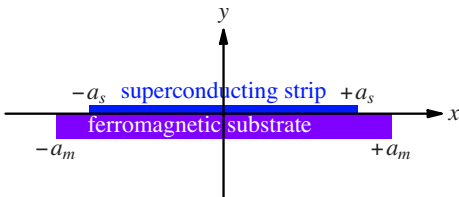


FIG. 6. (Color online) Cross section of a SC/FM strip with a wider ferromagnetic substrate. The superconducting strip is situated at $|x| < a_s$ and $0 < y < d_s$, and the ferromagnetic substrate is at $|x| < a_m$ and $-d_m < y < 0$, where $d_s + d_m \ll 2a_s < 2a_m$.

section field $\mu_0 H_0 \approx 0.14 \mu_0 j_c d_s$ is on the order of mT for typical coated conductors.

(iii) When the ferromagnetic substrate is wider than the superconducting strip, χ'_1 of a SC/FM strip for $H_0/j_c d_s \lesssim 1$ is suppressed, and can be smaller than that of a SC/NM strip [Fig. 5(b)].

Suenaga *et al.*¹³ experimentally investigated the effects of ferromagnetic Ni-W alloy tapes on ac losses Q of YBa₂Cu₃O₇ coated conductors, and they confirmed that ac losses of ferromagnetic substrates are much smaller than those of superconducting strips (see also Refs. 7 and 10). The above theoretical predictions (i) and (ii) agree well with these experimental data. The theoretical intersection field $\mu_0 H_0 \approx 0.14 \mu_0 j_c d_s$ of χ''_1 vs H_0 (or Q vs H_0) described in the prediction (ii) is estimated to be about 4.9 mT for $j_c = 1.2 \times 10^{10}$ A/m² and $d_s = 2.3$ μ m, which agrees well with the experimental data by Suenaga *et al.*¹³

Prediction (iii) clearly explains that the enhancement of χ''_1 of a SC/FM strip with $a_m/a_s = 1$ when $H_0/j_c d_s < 0.14$ is due to the edge effect of a ferromagnetic substrate. The edges effects are also seen in Fig. 3(b) (i.e., the intersection of the lines of b_0 vs H_0) and in Fig. 4(a) (i.e., the intersection of H_y vs x).

Although our simple model for ferromagnetic substrates assumes an infinite permeability ($\mu_m/\mu_0 \rightarrow \infty$) in contrast to $\mu_m/\mu_0 \sim 30$ in a Ni-W alloy used in coated conductors,¹³ the quantitative agreement of our theoretical predictions with the experimental data by Suenaga *et al.* suggests that the ideal soft magnet model with an infinite permeability works well when $\mu_0/\mu_m \ll 1$.^{11,13,14,34}

In summary, analytical expressions of the complex field were derived for SC/FM strips. The ferromagnetic substrates were regarded as ideal soft magnets with an infinite permeability, and the critical state model was used to calculate the magnetic moment and ac susceptibility of a SC/FM strip exposed to a perpendicular magnetic field. The theoretical results of the ac susceptibility of a SC/FM strip exposed to a perpendicular magnetic field agreed well with the experimental data by Suenaga *et al.*¹³

ACKNOWLEDGMENT

I thank M. Suenaga for stimulating discussions about his experimental data prior to its publication.

APPENDIX A: DERIVATION OF THE COMPLEX FIELD

In this appendix, we derive Eqs. (13), (18), and (23). The relationship between the complex potential $\mathcal{G}(\zeta)$ in the ζ plane and $\tilde{\mathcal{G}}(\eta)$ in the η plane is simply given by²⁰ $\mathcal{G}(\zeta) = \tilde{\mathcal{G}}(\eta)$. The complex field $\mathcal{H}(\zeta) = d\mathcal{G}(\zeta)/d\zeta$ in the ζ plane is, therefore, obtained from the complex field $\tilde{\mathcal{H}}(\eta) = d\tilde{\mathcal{G}}(\eta)/d\eta$ in the η plane as

$$\mathcal{H}(\zeta) = \tilde{\mathcal{H}}(\eta) \frac{d\eta}{d\zeta} = \tilde{\mathcal{H}}(\eta) \frac{i\sqrt{\eta^2 - a^2}}{\eta}, \quad (\text{A1})$$

where we used Eq. (10).

When $H_{ay} \neq 0$ and $H_{ax}=I_z=0$ as in Sec. III A, the complex field in the η plane is similar to that for a superconducting strip [situated at $0 < \text{Re}(\eta) < a$ and $\text{Im}(\eta)=0$] exposed to a magnetic field,^{16,17,25}

$$\tilde{\mathcal{H}}(\eta) = -iH_{ay} \frac{\eta - a/2}{\sqrt{\eta(\eta - a)}}. \quad (\text{A2})$$

Substitution of Eq. (A2) into Eq. (A1) yields Eq. (13).

When $H_{ax} \neq 0$ and $H_{ay}=I_z=0$ as in Sec. III B, the complex field in the η plane corresponds to that for a superconducting strip [situated at $-a < \text{Re}(\eta) < 0$ and $\text{Im}(\eta)=0$] exposed to a magnetic field,^{16,17,25}

$$\tilde{\mathcal{H}}(\eta) = H_{ax} \frac{\eta + a/2}{\sqrt{\eta(\eta + a)}}. \quad (\text{A3})$$

Substitution of Eq. (A3) into Eq. (A1) yields Eq. (18).

When $I_z \neq 0$ and $H_{ay}=H_{ax}=0$ as in Sec. III C, the complex field in the η plane corresponds to that for a superconducting strip [situated at $-a < \text{Re}(\eta) < 0$ and $\text{Im}(\eta)=0$] carrying a transport current,^{16,17,22}

$$\tilde{\mathcal{H}}(\eta) = \frac{I_z}{2\pi} \frac{1}{\sqrt{\eta(\eta + a)}}. \quad (\text{A4})$$

Substitution of Eq. (A4) into Eq. (A1) yields Eq. (23).

APPENDIX B: SQUARE ROOT FUNCTIONS

When we consider the behavior of $\mathcal{H}(\zeta)$ and $\mathcal{G}(\zeta)$ that contain square root functions, it is necessary to take care of the branch lines (i.e., cut lines) of the square root functions. The branch lines of the square root functions are shown, for example, in Ref. 35: the branch line of $\sqrt{\zeta}$ is on the real axis of $-\infty < \text{Re}(\zeta) < 0$, and the branch line of $\sqrt{\zeta^2 - a^2}$ is on the real axis of $-a < \text{Re}(\zeta) < +a$.

Substitution of $\zeta = x \pm i\epsilon$ (where $\epsilon \rightarrow +0$) into Eq. (10) yields

$$\eta = \mp \sqrt{a^2 - x^2} \quad \text{when } \zeta = x \pm i\epsilon \quad (\text{B1})$$

for $|x| < a$. The square root functions in Eqs. (13), (18), and (23) are reduced to

$$\sqrt{(\eta + a)/\eta} = -i \text{sgn}(x) f_-(x), \quad (\text{B2})$$

$$i\sqrt{(\eta - a)/\eta} = i f_+(x), \quad (\text{B3})$$

when $\zeta = x + i\epsilon$ for $|x| < a$, where $\text{sgn}(x) = +1$ for $x > 0$, $\text{sgn}(x) = -1$ for $x < 0$, and

$$f_{\pm}(x) = \sqrt{\frac{a}{\sqrt{a^2 - x^2}} \pm 1}. \quad (\text{B4})$$

From Eqs. (B1)–(B3), we readily verify that Eqs. (13), (18), and (23) satisfy the boundary condition of Eq. (12). The square root functions are reduced to

$$\sqrt{(\eta + a)/\eta} = -f_+(x), \quad (\text{B5})$$

$$i\sqrt{(\eta - a)/\eta} = -\text{sgn}(x) f_-(x), \quad (\text{B6})$$

when $\zeta = x - i\epsilon$ for $|x| < a$. From Eqs. (B1), (B5), and (B6), we also verify that Eqs. (13), (18), and (23) satisfy Eq. (11).

APPENDIX C: SUPERCONDUCTING STRIP ON A WIDE FERROMAGNETIC SUBSTRATE

The complex field for a SC/FM strip in which the ferromagnetic substrate is wider than the superconducting strip^{6,12} (i.e., $2a_m > 2a_s$, as shown in Fig. 6) is derived here. The SC/FM strip carries no net transport current and is exposed to a perpendicular magnetic field $H_{ay} = H_0$, and the superconducting strip is in the critical state.

The boundary condition at the surface of the ferromagnetic substrate is given by

$$H_x(x, -\epsilon) = \text{Im } \mathcal{H}(x - i\epsilon) = 0 \quad \text{for } |x| < a_m. \quad (\text{C1})$$

On the basis of the critical state model, the boundary conditions at the surface of a superconducting strip are

$$H_x(x, +\epsilon) = \text{Im } \mathcal{H}(x + i\epsilon) = -\text{sgn}(x) j_c d_s \quad \text{for } b_0 < |x| < a_s, \quad (\text{C2})$$

$$H_y(x, +\epsilon) = \text{Re } \mathcal{H}(x + i\epsilon) = 0 \quad \text{for } |x| < b_0, \quad (\text{C3})$$

where b_0 is the parameter for the flux front. The corresponding complex field, which satisfies Eqs. (C1)–(C3), is given by

$$\begin{aligned} \frac{\mathcal{H}(\zeta)}{2j_c d_s / \pi} = & \text{arctanh} \left[\sqrt{\frac{(\beta_0 - \alpha_s)(\eta + a_m)}{(a_m - \alpha_s)(\eta + \beta_0)}} \right] \\ & - \frac{\sqrt{(a_m - \alpha_s)(\beta_0 - \alpha_s)(\eta + a_m)(\eta + \beta_0)}}{(a_m + \beta_0)\eta}, \end{aligned} \quad (\text{C4})$$

where

$$\alpha_s = \sqrt{a_m - a_s}, \quad \beta_0 = \sqrt{a_m - b_0}. \quad (\text{C5})$$

The parameter β_0 is related to H_0 as

$$\frac{H_0}{2j_c d_s / \pi} = \text{arctanh} \left(\sqrt{\frac{\beta_0 - \alpha_s}{a_m - \alpha_s}} \right) - \frac{\sqrt{(a_m - \alpha_s)(\beta_0 - \alpha_s)}}{a_m + \beta_0}. \quad (\text{C6})$$

The magnetic moment per unit length, $m_y = m_0(H_0)$, is

$$\frac{m_0}{j_c d_s} = - \left(\frac{2a_m \beta_0}{a_m + \beta_0} + \alpha_s \right) \sqrt{(a_m - \alpha_s)(\beta_0 - \alpha_s)}. \quad (\text{C7})$$

The differential susceptibility is simply given by

$$\frac{\partial m_0}{\partial H_0} = - \frac{\pi}{4} (3a_m + \beta_0)(a_m - \beta_0). \quad (\text{C8})$$

For $H_0 \ll j_c d_s$ (i.e., $\beta_0 \approx \alpha_s$), Eq. (C8) is reduced to

$$\frac{\partial m_0}{\partial H_0} \approx - \frac{\pi}{4} (2a_m^2 + a_s^2 - 2a_m \sqrt{a_m^2 - a_s^2}), \quad (\text{C9})$$

which is further simplified to $\partial m_0 / \partial H_0 \approx -(\pi/2)a_s^2$ for $a_m \gg a_s$.

The ac susceptibility of SC/FM strips with wider ferromagnetic substrates can be calculated by substituting Eqs. (C6) and (C7) into Eq. (39). The calculated results for χ_1'' are shown as dotted lines in Fig. 5(b).

- ¹Y. Shiohara, M. Yoshizumi, T. Izumi, and Y. Yamada, *Physica C* **463-465**, 1 (2007).
- ²A. Goyal, D. P. Norton, J. D. Budai, M. Paranthaman, E. D. Specht, D. M. Kroeger, D. K. Christen, Q. He, B. Saffian, F. A. List, D. F. Lee, P. M. Martin, C. E. Klabunde, E. Hartfield, and V. L. Sikka, *Appl. Phys. Lett.* **69**, 1795 (1996).
- ³A. O. Ijaduola, J. R. Thompson, A. Goyal, C. L. H. Thieme, and K. Marken, *Physica C* **403**, 163 (2004).
- ⁴R. C. Duckworth, J. R. Thompson, M. J. Gouge, J. W. Lue, A. O. Ijaduola, D. Yu, and D. T. Verebelyi, *Supercond. Sci. Technol.* **16**, 1294 (2003).
- ⁵O. Tsukamoto, H. Nakayama, S. Okada, M. Ciszek, S. Hahakura, M. Umeyama, K. Ohmatsu, and D. Miyagi, *Physica C* **426-431**, 1290 (2005).
- ⁶F. Gömöröy, J. Šouc, M. Vojenčiak, E. Seler, B. Klinčok, J. M. Ceballos, E. Pardo, A. Sanchez, C. Navau, S. Farinon, and P. Fabricatore, *Supercond. Sci. Technol.* **19**, S60 (2006).
- ⁷M. Suenaga, and Q. Li, *Appl. Phys. Lett.* **88**, 262501 (2006).
- ⁸J. H. Claassen, *Supercond. Sci. Technol.* **20**, 35 (2007).
- ⁹D. N. Nguyen, P. V. P. S. S. Sastry, and J. Schwartz, *J. Appl. Phys.* **101**, 053905 (2007).
- ¹⁰O. Tsukamoto, M. Liu, S. Odaka, D. Miyagi, and K. Ohmatsu, *Physica C* **463-465**, 766 (2007); O. Tsukamoto, S. Sekizawa, A. K. M. Alamgir, and D. Miyagi, *ibid.* **463-465**, 770 (2007).
- ¹¹N. Amemiya and M. Nakahata, *Physica C* **463-465**, 775 (2007).
- ¹²D. Miyagi, Y. Amadutsumi, N. Takahashi, and O. Tsukamoto, *Physica C* **463-465**, 781 (2007).
- ¹³M. Suenaga, M. Iwakuma, T. Sueyoshi, T. Izumi, M. Mimura, Y. Takahashi, and Y. Aoki (unpublished).
- ¹⁴Yu. A. Genenko, A. Usoskin, and H. C. Freyhardt, *Phys. Rev. Lett.* **83**, 3045 (1999); Yu. A. Genenko, A. Snezhko, and H. C. Freyhardt, *Phys. Rev. B* **62**, 3453 (2000).
- ¹⁵M. R. Halse, *J. Phys. D* **3**, 717 (1970).
- ¹⁶E. H. Brandt, M. V. Indenbom, and A. Forkl, *Europhys. Lett.* **22**, 735 (1993); E. H. Brandt and M. Indenbom, *Phys. Rev. B* **48**, 12893 (1993).
- ¹⁷E. Zeldov, J. R. Clem, M. McElfresh, and M. Darwin, *Phys. Rev. B* **49**, 9802 (1994).
- ¹⁸L. D. Landau and E. M. Lifschitz, *Electrodynamics of Continuous Media*, Theoretical Physics Vol. 8 (Pergamon, Oxford, 1963).
- ¹⁹R. A. Beth, *J. Appl. Phys.* **37**, 2568 (1966).
- ²⁰J. R. Clem, R. P. Huebener, and D. E. Gallus, *J. Low Temp. Phys.* **12**, 449 (1973).
- ²¹E. Zeldov, A. I. Larkin, V. B. Geshkenbein, M. Konczykowski, D. Majer, B. Khaykovich, V. M. Vinokur, and H. Shtrikman, *Phys. Rev. Lett.* **73**, 1428 (1994).
- ²²Y. Mawatari and J. R. Clem, *Phys. Rev. Lett.* **86**, 2870 (2001).
- ²³A. A. Babaei Brojeny, Y. Mawatari, M. Benkraouda, and J. R. Clem, *Supercond. Sci. Technol.* **15**, 1454 (2002).
- ²⁴E. B. Sonin, *Phys. Rev. B* **66**, 136501 (2002).
- ²⁵Y. Mawatari and J. R. Clem, *Phys. Rev. B* **68**, 024505 (2003).
- ²⁶Y. Mawatari and J. R. Clem, *Phys. Rev. B* **74**, 144523 (2006).
- ²⁷J. R. Clem and Y. Mawatari, *Phys. Rev. B* **74**, 214505 (2006).
- ²⁸G. B. Arfken and H. J. Weber, *Mathematical Methods for Physicists*, 5th ed. (Harcourt, Brace, New York, /Academic, San Diego, 2001).
- ²⁹J. D. Jackson, *Classical Electrodynamics*, 2nd ed. (Wiley, New York, 1975).
- ³⁰C. P. Bean, *Phys. Rev. Lett.* **8**, 250 (1962); *Rev. Mod. Phys.* **36**, 31 (1964).
- ³¹E. H. Brandt, *Phys. Rev. B* **55**, 14513 (1997).
- ³²Equations (35) and (36) come from the fact that the evolution of the complex field is given by (Refs. 15–17) $\mathcal{H}(\zeta, t) = \pm \mathcal{H}_0(\zeta, H_0) \mp 2\mathcal{H}_0(\zeta, H_0(1 \mp \cos \omega t)/2)$, where $\mathcal{H}_0(\zeta, H_0)$ corresponds to Eq. (29). The resulting complex field $\mathcal{H}(\zeta, t)$ satisfies the boundary condition of Eq. (11) at the surface of the ferromagnetic substrate, and is valid for SC/FM strips exposed to ac magnetic fields.
- ³³J. R. Clem and A. Sanchez, *Phys. Rev. B* **50**, 9355 (1994).
- ³⁴The validity of the infinite-permeability model may be subject to the restriction due to the geometry of the ferromagnetic substrates, as shown in Yu. A. Genenko and A. V. Snezhko, *J. Appl. Phys.* **92**, 357 (2002); Yu. A. Genenko, A. V. Snezhko, and A. Usoskin, *Physica C* **401**, 236 (2004), see also Ref. 8.
- ³⁵P. M. Morse and H. Feshbach, *Methods of Theoretical Physics* (McGraw-Hill, New York, 1953), Pt. 1, Chap. 4.